Experimental Demonstration of a 40 Mb/s VLC System Using a Large Off-the-Shelf LED Panel

Xicong Li
Optical Communications Research Group
Northumbria University
Newcastle upon Tyne, NE1 8ST, UK
xicong.li@northumbria.ac.uk

Zabih Ghassemlooy
Optical Communications Research Group
Northumbria University
Newcastle upon Tyne, NE1 8ST, UK
z.ghassemlooy@northumbria.ac.uk

Stanislav Zvanovec
Department of Electromagnetic Field
Czech Technical University in Prague
Prague, 16627, Czech Republic
xzvanove@fel.cvut.cz

Paul Anthony Haigh
Intelligent Sensing and Communications Group
Newcastle University
Newcastle upon Tyne, NE1 7RU, UK
Paul.Haigh@newcastle.ac.uk

***Abstract*—This paper experimentally demonstrates a VLC system using a large off-the-shelf LED panel with dimensions of 60$\times$60 cm^2 and achieves a data rate of 40 Mb/s based on multi-band carrier-less amplitude and phase (CAP) modulation. The proposed system demonstrates the potential of utilising the existing LED-based lighting infrastructure for simultaneous indoor illumination and data communication.**

***Index Terms*—VLC, LED, carrier-less amplitude and phase modulation, multi-carrier modulation, bit-loading**

I. Introduction

Visible light communications (VLC) has been proposed as a promising technology because it offers a large unlicensed spectrum outside the congested radio spectrum, with no interference with existing radio-frequency infrastructure, alongside inherent security due to light confinement to a room [1], [2]. Meanwhile, VLC systems can reuse the existing solid-state light-emitting diode (LED)-based lighting infrastructure, thus reducing the deployment cost significantly [3]. In addition, the maturity of power line communications (PLC) [4] help facilitate the cable installation of VLC systems, where the existing power line cables will deliver both power and data at the same time [5].

Motivated by the advantages and market potential of VLC, standardisation has been carried out by several organisations [6]–[8]. In 2007, Japan Electronics and Information Technology Industries Association (JEITA) pioneered standards focusing on low-rate visible ID systems. In 2008, the Visible Light Communication Consortium (VLCC) forged an alliance with the Infrared Data Association (IrDA) and published IrDA-type standards for VLC. In 2009, the task group IEEE 802.15.7 was established to work on a novel VLC standard covering both physical (PHY) and media access control (MAC) layer. In 2017, a new task group IEEE 802.15.13 was split from the former group and continued working on high-rate communication based on photodiodes. In 2018, IEEE 802.11bb Light Communications Task Group was formed with its intent to develop a global standard for light communications within the well-known WIFI standard family. This group aims to provide 10 Mb/s to 5 Gb/s connection using light spectrum from 380 to 5000 nm. To date, IEEE has not released completed standards on high-speed VLC. Recently, ITU-T published the latest G.9961 Recommendation (previous G.vlc) [9] which defines two PHY specification based on orthogonal frequency division multiplex (OFDM) supporting three baseband modulation bandwidth of 50, 100 and 200 MHz. It is worth mentioning that G.9961 PHY I is based on G.9960 [10], which is also known as G.hn and is one of the popular standards for high-speed power line communication. Refer to [11] for further information about the above standards.

The ability to reuse existing lighting infrastructure is a key advantage for VLC to gain popularity in the massive consumer market, especially in an indoor home and office environment. However, white phosphorous LEDs for general illuminance typically have a 3-dB bandwidth in the region of several MHz, thus imposing a limitation on the achievable information rate. Multi-carrier modulation [10] is a solution to this issue. The signal bandwidth can go beyond the LED's 3-dB bandwidth because it is divided into many narrow quasi-flat sub-bands which can tolerate out-of-band attenuation. One of the popular multi-carrier modulation schemes is OFDM which can be efficiently realised by using the fast Fourier transform (FFT). However, OFDM suffers from a high peak-to-average power ratio (PAPR), especially when using a large number of subcarriers. The simplest method to mitigate high PAPR is to limit the peak amplitude to a certain level, which inevitably introduces clipping noise and degrade the bit error rate (BER) [12].

Another multi-carrier modulation format is multi-band carrier-less amplitude and phase (MultiCAP) modulation, the time series of which is the accumulation of multiple frequency-separated single-carrier CAP signals [13]–[16]. Since the number of subcarriers in MultiCAP is typically much smaller than OFDM, MultiCAP has a lower PARP. In addition, it has been experimentally confirmed in [16] that MultiCAP outperforms OFDM in terms of data rates at the same required BER level, across the same physical link. Therefore, in this paper, we select MultiCAP to demonstrate the achievable transmission speed of a VLC system which utilises the existing lighting infrastructure with minor modification.

We experimentally show that 40 Mb/s MultiCAP can be supported with a 7% forward error correction (FEC) code in the distance range up to 200 cm without extra focus and filter optics.

The rest of the paper is organised as follow. Section II characterises the off-the-shelf LED panel in use and provides a modulation circuit to modulate the intensity of the panel. Section III describes the modulation scheme and communication system design. Section IV gives the experimental results. Finally, the conclusion is made in Section V.

II. LED Panel Characteristics

We start by characterising the commercial LED panel under test and then design the modulation circuit accordingly.

A. V-I Characteristics

As depicted by the section view of the LED panel in Fig. 1(a), a string of LEDs are installed on two sides of the square aluminium frame and the light emitted from those LEDs are directed through a transparent light guide. On top of the light guide is one layer of reflective paper, which prevents the light from escaping in the unwanted direction, while the other side of the light guide is a diffuser plate to distribute the light as evenly as possible for illumination.

The core of the LED panel in use is a string of LEDs wired both in series and in parallel. The schematic of our LED panel in Fig. 1(b) shows that it has 12 blocks connected in series, each of which consists of 20 parallel white LEDs. The measured *V-I* curve of the LED string as an lumped element is shown in Fig. 2.

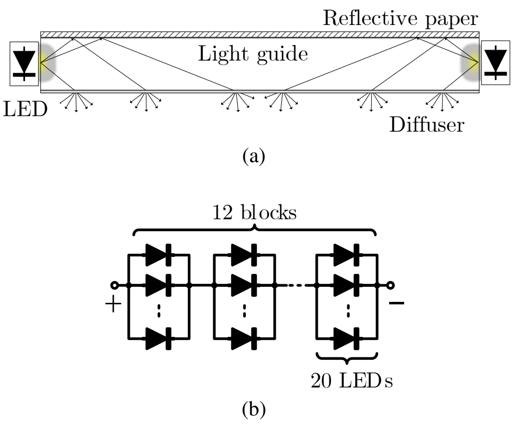

Fig. 1: (a) Section view and (b) schematic of the LED panel in use.

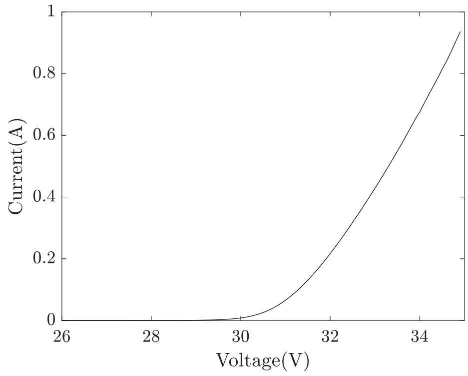

Fig. 2: Measured *V-I* curve of the LED panel.

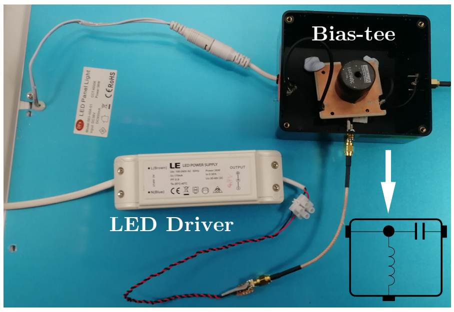

Fig. 3: Bias-tee driving the LED panel.

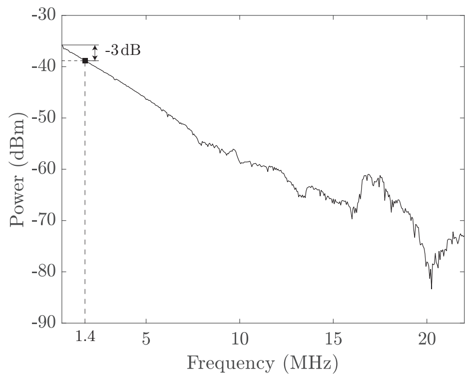

Fig. 4: Measured frequency response of the LED panel.

B. Modulation Circuit Design and Frequency Response

A key challenge in using the existing lighting sources as an optical transmitter is how to combine information carrying AC signals with the DC bias signal generated by an independent driver which is normally provided along with the LED panel by the manufacturer. Here, we designed a bias-tee which consists of only a capacitor and an inductor, see Fig. 3, to achieve the minimum degree of modification and minimise additional deployment costs.

With the bias-tee, the frequency response of the LED panel is measured and plotted in Fig. 4. From the curve, a 3-dB bandwidth of 1.4 MHz can be determined. It is also evident that the LED panel exhibits severe distortion beyond 10 MHz, which degrades the BER performance of sub-bands utilising spectrum in this frequency range. Based on the observation, we set the modulation bandwidth to 10 MHz to avoid the detrimental effect of distortion.

III. System Design

A. System Block Diagram

The block diagram of the proposed system is shown in Fig. 5. The key system parameters are provided in Table I. We generate waveforms in MATLAB following the modulation scheme, which is discussed in detail later, and upload the signals to the arbitrary waveform generator (AWG) for intensity modulation of the LED panel via the bias-tee. The LED panel is installed in the ceiling as in real-world office scenarios. The optical receiver is placed directly under the light source and connected to an oscilloscope (OSC) which captures data to process offline in MATLAB.

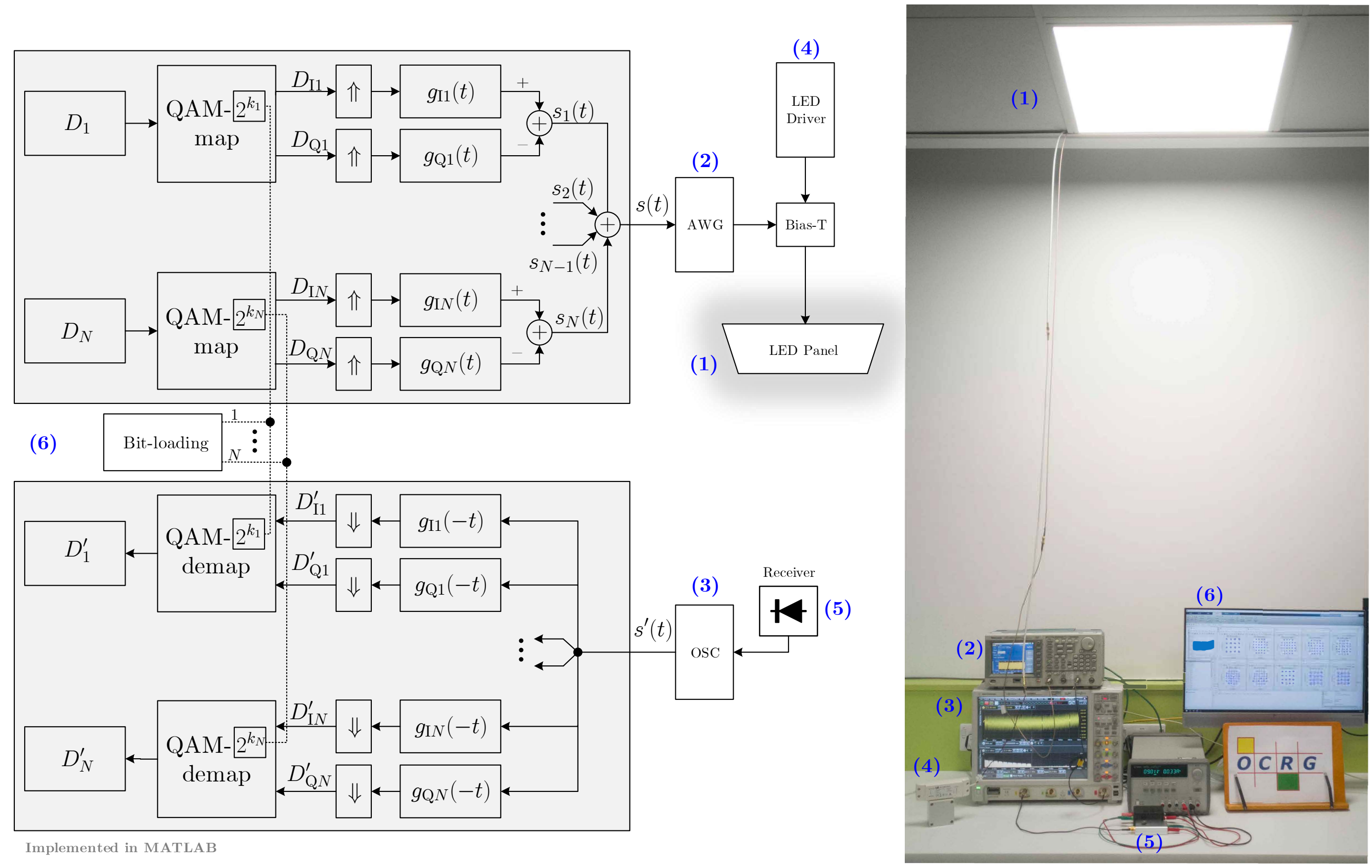

(a) (b)

Fig. 5: (a) System block diagram, (b) experimental setup.

Our optical receiver uses a photodiode with a detection area of 7×7 mm^2 and a half angle of 70° to eliminate the need for bulky optics and precise alignment, which is essential for practical applications. Measurement shows that our receiver has a 3-dB bandwidth of 20 MHz [1].

TABLE I: Key system parameters

Parameter	Value
LED panel	DFx 563-004-01, 4000K, biased at 0.9 A
Photodiode	Hamamatsu, S6968, 320 to 1060 nm
Transimpedance amplifier	Analog AD8015, 10 kΩ gain (single ended)
Oscilloscope	Keysight DSO9254A, 2.5 GSample/sec
Function generator	Tektronix AFG3022, 10 Vpp
Modulation bandwidth	$B_{\mathrm{mod}} = 10$ MHz
DAC sampling rate	40 MSample/sec
Carrier number	$N = 10$
SRRC rolloff factor	$\beta = 0.15$
SRRC filter length	20 symbols
Carrier frequency	0.5 to 9.5 MHz with a step size of 1 MHz
Baseband symbol rate	$1/T_s = 869.57$ kBaud
Bit-loading pattern	4 5 5 5 5 5 5 4 4 4
Aggregate data rate	40 Mb/s

[1]The receiver's bandwidth is tested with a laser diode with a bandwidth > 100 MHz. Therefore, the measured frequency response in Fig. 4 mainly represents the LED panel because its bandwidth is dominant in the entire system.

B. Modulation Scheme

This section briefly reviews the principle of the MultiCAP modulation scheme and describes how the demodulation algorithm works [14].

At the transmitter, a random binary sequence $\{D_n\}$ is mapped into the QAM-2^{k_n} constellation, where k_n is the number of bits-per-symbol loaded onto the n-th sub-carrier at a caririer frequency $f_n = \frac{2n-1}{2N} B_{\mathrm{mod}}$, $n = 1, \ldots, N$, where N is the number of sub-carriers and B_{mod} is the modulation bandwidth. After the constellation mapping, $\{D_n\}$ is split into its in-phase $\{D_{\mathrm{I}n}\}$ and quadrature $\{D_{\mathrm{Q}n}\}$ components. Then $\{D_{\mathrm{I}n}\}$, $\{D_{\mathrm{Q}n}\}$ are upsampled and convolved with their respective in-phase and quadrature filters [17] given by:

$$g_{\mathrm{I}n}(t) = g(t) \sin 2\pi f_n t$$
$$g_{\mathrm{Q}n}(t) = g(t) \cos 2\pi f_n t$$

to form each sub-carrier CAP signal, which is given by:

$$s_n(t) = D_{\mathrm{I}n} \circledast g_{\mathrm{I}n}(t) - D_{\mathrm{Q}n} \circledast g_{\mathrm{Q}n}(t).$$

$g(t)$ is the square-root raised cosine (SRRC) pulse given by:

$$g(t) = \frac{\sin[\pi(1-\beta)t/T_s] + 4\beta t/T_s \cos[\pi(1+\beta)t/T_s]}{\pi t/T_s \left[1 - (4\beta t/T_s)^2\right]},$$

where $0 < \beta < 1$ is the roll-off factor, $\circledast$ denotes time-domain convolution, and $T_s = N(1+\beta)/B_{\mathrm{mod}}$ is the symbol period for transmitting $\{D_{\mathrm{I}n}\}$, $\{D_{\mathrm{Q}n}\}$. Finally, all sub-band signals are summed up to generate the multi-band signal as given by:

$$s(t) = \sum_{n=1}^{N} s_n(t).$$

At the receiver, the received signal $s'(t)$ is convolved with $2N$ matched filters with the pulse response of $g_{\mathrm{I}n}(-t)$ and $g_{\mathrm{Q}n}(-t)$ followed by downsampling in order to recover $\{D'_{\mathrm{I}n}\}$ and $\{D'_{\mathrm{Q}n}\}$. The symbols $\{D'_{\mathrm{I}n}\}$ and $\{D'_{\mathrm{Q}n}\}$ are then demapped to recover an estimate of the data $\{D'_n\}$ for element-wise BER testing.

In bit loading, the largest number of bits-per-symbol for each sub-carrier k_n is calculated given a maximum BER level. In this paper, this process is carried out recursively by offline BER measurement in a bit-by-bit manner in order to find the largest constellation for each sub-carrier below a BER of $3.8{\times}10^{-3}$ (i.e., the 7% FEC limit).

IV. Results

In Fig. 6, the measured BER is illustrated as a function of the distance between the LED panel and the receiver. A 40 Mb/s link can be supported up to 200 cm, maintaining BER performance below the 7% FEC limit level. However, in an office environment, a light level of 600 lux is required at desk height [17], which means the distance had to be decreased to 140 cm to obtain this light level, as highlighted by the marker in Fig. 6. Therefore, the system has a degree of flexibility and can tolerate light levels beneath 600 lux at the 40 Mb/s data rate.

The corresponding signal spectrum is plotted in Fig. 7 together with the noise spectrum, which provide an estimate of the signal-to-noise ratio (SNR) of each sub-carrier. In addition, the insets in Fig. 7 provides the constellation diagram of each sub-carrier as supportive information.

Some limitations exist in our proposed system. One critical problem is the flickering caused by the residual current ripple provided by the LED panel driver. This slowly-changing component in light intensity should be filtered out from the received signal to guarantee a relatively stable signal amplitude. Another problem is the limited bandwidth of the existing LED lighting devices, which hinders the application of the emerging high-speed VLC standards in the real world.

V. Conclusion

We experimentally demonstrated a 40 Mb/s VLC system using a large commercial LED panel with minor modification. The possibility of reusing the existing LED-based lighting infrastructure in VLC applications had been confirmed.

Acknowledgment

This work is supported by the European Union's Horizon 2020 research and innovation programme under the Marie Skłodowska-Curie grant agreement no 764461 (VISION) and the EPSRC UK Grant MARVEL (EP/P006280/1).

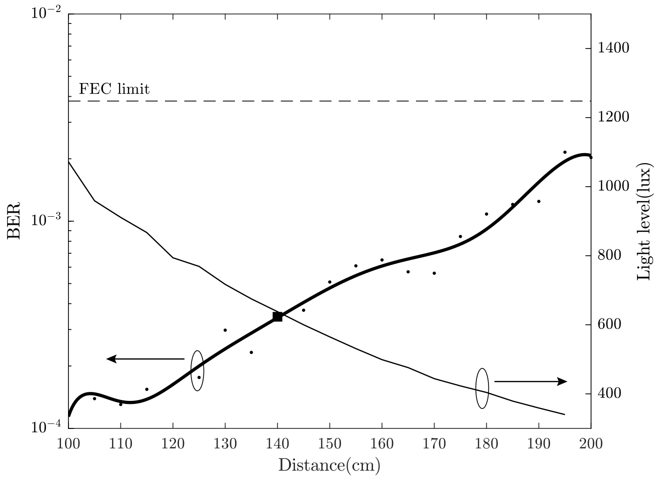

Fig. 6: BER and light level vs distance.

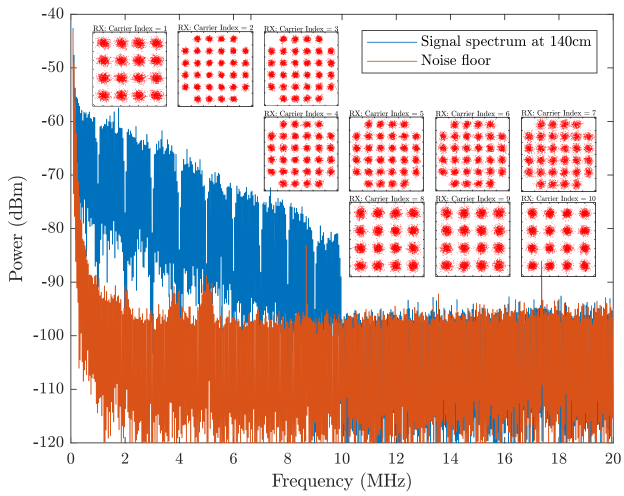

Fig. 7: Measured spectra at a distance of 140 cm.

References

[1] Z. Ghassemlooy, L. N. Alves, S. Zvanovec, and M.-A. Khalighi, *Visible Light Communications: Theory and Applications*. CRC Press, 2017.

[2] M. Uysal, C. Capsoni, Z. Ghassemlooy, A. Boucouvalas, and E. Udvary, *Optical Wireless Communications: An Emerging Technology*. Springer, 2016.

[3] S. Pimputkar, J. S. Speck, S. P. DenBaars, and S. Nakamura, "Prospects for LED lighting," *Nature Photonics*, vol. 3, no. 4, pp. 180–182, 2009. [Online]. Available: https://doi.org/10.1038/nphoton.2009.32

[4] S. Galli, A. Scaglione, and Z. Wang, "For the grid and through the grid: The role of power line communications in the smart grid," *Proceedings of the IEEE*, vol. 99, no. 6, pp. 998–1027, 2011.

[5] H. Ma, L. Lampe, and S. Hranilovic, "Integration of indoor visible light and power line communication systems," in *2013 IEEE 17th International Symposium on Power Line Communications and Its Applications*, 2013, Conference Proceedings, pp. 291–296.

[6] T. Nguyen, A. Islam, T. Yamazato, and Y. M. Jang, "Technical issues on IEEE 802.15.7m image sensor communication standardization," *IEEE Communications Magazine*, vol. 56, no. 2, pp. 213–218, 2018.

[7] V. Jungnickel, M. Uysal, N. Serafimovski, T. Baykas, D. O. Brien, E. Ciaramella, Z. Ghassemlooy, R. Green, H. Haas, P. A. Haigh, V. P. G. Jimenez, F. Miramirkhani, M. Wolf, and S. Zvanovec, "A European view on the next generation optical wireless communication standard," in *2015 IEEE Conference on Standards for Communications and Networking (CSCN)*, 2015, Conference Proceedings, pp. 106–111.

[8] S. Rajagopal, R. D. Roberts, and S. K. Lim, "IEEE 802.15.7 visible light communication: modulation schemes and dimming support," *IEEE Communications Magazine*, vol. 50, no. 3, pp. 72–82, 2012.

[9] *G.9961 : Unified high-speed wireline-based home networking transceivers - Data link layer specification*, International Telecommunication Union Telecommunication (ITU-T) Standardization Sector Std.

[10] V. Oksman and S. Galli, "G.hn: The new ITU-T home networking standard," *IEEE Communications Magazine*, vol. 47, no. 10, pp. 138–145, 2009.

[11] V. Jungnickel, M. Hinrichs, K. L. Bober, C. Kottke, A. A. Corici, M. Emmelmann, J. Rufo, P. . Bök, D. Behnke, M. Riege, X. Wu, R. Singh, D. C. O'Brien, S. Collins, F. Faulkner, M. M. Vazquez, M. C. Bech, F. Geilhardt, R. . Braun, X. Deng, E. Tangdiongga, and A. M. J. Koonen, "Enhance lighting for the Internet of things," in *2019 Global LIFI Congress (GLC)*, June 2019, pp. 1–6.

[12] M. Khalighi, S. Long, S. Bourennane, and Z. Ghassemlooy, "PAM- and CAP-based transmission schemes for visible-light communications," *IEEE Access*, vol. 5, pp. 27 002–27 013, 2017.

[13] X. Li, Z. Ghassemlooy, S. Zvanovec, R. P. Jimenezz, and P. Haigh, "Should analogue pre-equalisers be avoided in VLC systems?" *IEEE Photonics Journal*, pp. 1–1, 2020.

[14] P. A. Haigh, A. Burton, K. Werfli, H. L. Minh, E. Bentley, P. Chvojka, W. O. Popoola, I. Papakonstantinou, and S. Zvanovec, "A Multi-CAP visible-light communications system with 4.85-b/s/Hz spectral efficiency," *IEEE Journal on Selected Areas in Communications*, vol. 33, no. 9, pp. 1771–1779, 2015.

[15] M. I. Olmedo, T. Zuo, J. B. Jensen, Q. Zhong, X. Xu, S. Popov, and I. T. Monroy, "Multiband carrierless amplitude phase modulation for high capacity optical data links," *Journal of Lightwave Technology*, vol. 32, no. 4, pp. 798–804, 2014.

[16] F. M. Wu, C. T. Lin, C. C. Wei, C. W. Chen, Z. Y. Chen, H. T. Huang, and S. Chi, "Performance comparison of OFDM signal and CAP signal over high capacity RGB-LED-based WDM visible light communication," *IEEE Photonics Journal*, vol. 5, no. 4, pp. 7 901 507–7 901 507, 2013.

[17] P. A. Haigh and I. Darwazeh, "Real time implementation of CAP modulation with 'better-than-Nyquist' pulse shaping in visible light communications," *IEEE Communications Letters*, pp. 1–1, 2020.